

Operational Safety Assessment of a High-Speed Train Exposed to the Strong Gust Wind

Mengge Yu^{1,2}, Zhenkuan Pan^{3,*}, Jiali Liu⁴ and Haiqing Li¹

Abstract: The operational safety characteristics of trains exposed to a strong wind have caused great concern in recent years. In the present paper, the effect of the strong gust wind on a high-speed train is investigated. A typical gust wind model for any wind angle, named “Chinese hat gust wind model”, was first constructed, and an algorithm for computing the aerodynamic loads was elaborated accordingly. A vehicle system dynamic model was then set up in order to investigate the vehicle system dynamic characteristics. The assessment of the operational safety has been conducted by means of characteristic wind curves (CWC). As some of the parameters of the wind-train system were difficult to measure, we also investigated the impact of the uncertain system parameters on the CWC. Results indicate that, the descending order of the operational safety index of the vehicle for each wind angle is 90° - 60° - 120° - 30° - 150° , and the worst condition for the operational safety occurs when the wind angle reaches around 90° . According to our findings, the gust factor and aerodynamic side force coefficient have great impact on the critical wind speed. Thus, these two parameters require special attention when considering the operational safety of a railway vehicle subjected to strong gust wind.

Keywords: Operational safety, high-speed train, gust wind, aerodynamic loads, characteristic wind curves.

1 Introduction

In recent years, the railway vehicle shows a trend of higher speed and lighter weight. This development is advantageous for energy consumption and acceleration, but very unfavorable for safe operation. Firstly, the high driving speed amplifies the aerodynamic performance of the train, especially for crosswind stability [Mao, Xi, Gao et al. (2014); Yan, Chen and Li (2018)]. Moreover, a lighter vehicle is more endangered by strong crosswind [Kikuchi and Suzuki (2015)]. The topic of crosswind stability of railway vehicle has caused much concern in recent years. The assessment of the wind stability of

¹ Postdoctoral Research Station of System Science, College of Automation and Electrical Engineering, Qingdao University, Qingdao, 266071, China.

² College of Mechanical and Electronic Engineering, Qingdao University, Qingdao, 266071, China.

³ College of Computer Science & Technology, Qingdao University, Qingdao, 266071, China.

⁴ CRRC Qingdao Sifang Co., Ltd., Qingdao, 266111, China.

* Corresponding Author: Zhenkuan Pan. Email: zkpan@126.com.

Received: 26 June 2019; Accepted: 16 August 2019.

a railway vehicle consists of the aerodynamic characteristics and the vehicle system dynamic characteristics. Dorigatti et al. undertook the static and moving experiments so as to analyze the aerodynamic characteristics of the train when subjected to crosswind, and gave detailed pressure measurements on the train nose [Dorigatti, Sterling, Baker et al. (2015)]. Munoz-Paniagua et al. investigated the influence of EARSM, SAS and IDDES turbulence models on the train aerodynamics (aerodynamic force coefficients, pressure distribution, flow structure, etc.) under crosswind [Munoz-Paniagua, García and Lehugeur (2017)]. Cheli et al. combined wind tunnel test and numerical calculation so as to obtain the optimal train shape in terms of crosswind stability [Cheli, Ripamonti and Rocchi (2010)]. The aerodynamic loads are then input into a dynamic model of the train to evaluate the characteristic wind curves (CWC), which is a series of wind speeds that the vehicle can tolerate before exceeding the permissible values of the safety index. Giappino et al. measured the aerodynamic force coefficients of a railway vehicle exposed to crosswinds, and evaluated the overturning risks based on the static equilibrium [Giappino, Rocchi, Schito et al. (2016)]. Chen et al. set up a dynamic model of the wind-train-rail system and discussed the dynamic performance [Chen and Xu (2014)].

In the crosswind stability analysis of the vehicle, the accurate simulation of natural wind is critical for the evaluation results. In most of the work mentioned above, the crosswind stability analysis was performed using a steady wind flow. The steady wind cannot reflect the transient characteristics of real wind. Therefore, a statistically typical gust has gained much attention, which is defined as an analytical function of time. In EN 14067-6 [EN 14067-6 (2010)], a gust wind model obtained by meteorological measurements, was depicted specifically. Kozmar et al. experimentally measured the unsteady aerodynamic loads of a train operating on a bridge exposed to gusty bora winds [Kozmar, Butler and Kareem (2012)]. Lv studied the aerodynamic performance of a high-speed train using different gust models, and evaluated the operational safety of the train based on multi-body dynamics theory [Lv (2016)]. Li et al. analyzed the dynamic characteristics of a railway vehicle under wind shear condition, and found that the safety indexes increased when the time interval of the wind shear decreased [Li, Zhang, Zou et al. (2014)]. However, in most of the previous study, the wind velocity was assumed to be normal to the track (the wind angle is 90°), and the variation of the wind direction was usually neglected. Moreover, some of the parameters of the wind-train system, such as the gust factor, gust duration, aerodynamic coefficients, usually have a relatively low precision for measurement or CFD calculation. The uncertainties and variability of the system parameters are normally neglected. A systematic analysis of the operational safety characteristics of the train subjected to a gust needs to be performed. Therefore, in this study, a typical gust wind model applied to any wind direction is constructed to conduct the operational safety evaluation of a railway vehicle. In particular, uncertain system parameters, such as the aerodynamic force/moment coefficients, gust duration and gust factor are discussed to investigate their impact on the operational safety.

2 Gust wind model

The coordinate system of the gust wind is drawn in Fig. 1. The x -axis is parallel to track. The angle between main wind direction w and railway track is defined as the wind angle α . Turbulence produces disturbances to the amplitude and the direction of the wind. The

deviations from the main wind direction are described by the components w'_u and w'_v , which are parallel and perpendicular to the main wind direction, respectively.

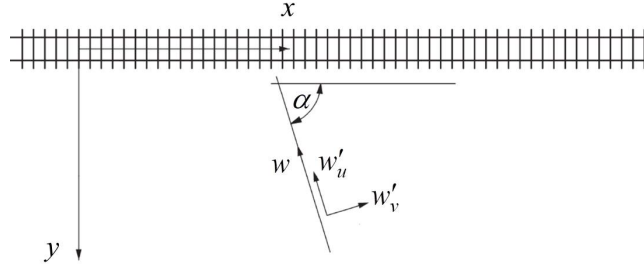


Figure 1: Coordinate system

The gust wind is a simplification of natural wind, and it can be defined by a function varying with time. Exponential shape is widely used as it is derived from the real wind data. The Chinese hat gust wind is an instance of the exponential shape [EN 14067-6 (2010)], which is shown in Fig. 2. In order to describe the fluctuating characteristics of gust wind, two parameters which are the gust factor and gust duration need to be defined.

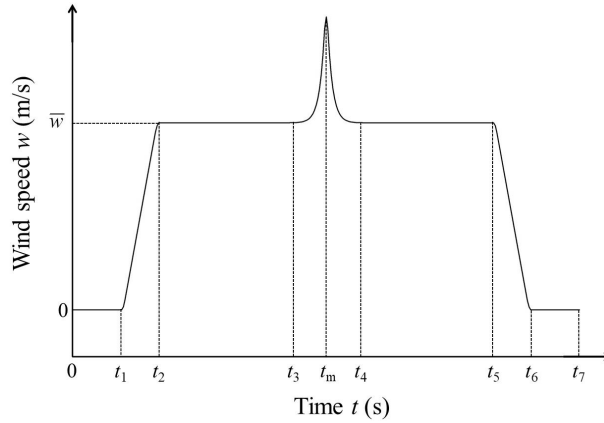


Figure 2: Gust wind scenario

The gust factor G is the ratio of peak wind speed \hat{w} to mean wind speed \bar{w}

$$G = \frac{\hat{w}}{\bar{w}} \tag{1}$$

The gust duration T can be computed by the power spectral density of natural wind, and the expression is [EN 14067-6 (2010)]

$$T = \frac{1}{2} \left(\frac{\int_{n_1}^{n_2} S_w(n) dn}{\int_{n_1}^{n_2} n^2 S_w(n) dn} \right)^{1/2} \tag{2}$$

where, $S_w(n)$ is the power spectral density of natural wind, n is frequency, n_1 and n_2 are

respectively lower and upper limit of frequency. The gust duration is a function mainly dependent on the mean wind speed, which can be solved numerically by performing a trapezoidal numerical integration using suitable resolution of the frequency range.

The von Karman spectral is adopted to simulate the wind characteristics, which is computed from:

$$\frac{nS_w(n)}{\sigma_w^2} = \frac{4(nL_w^x / \bar{w})}{\left(1 + 70.8(nL_w^x / \bar{w})^2\right)^{5/6}} \quad (3)$$

where, σ_w is standard deviation of the wind speed; L_w^x is the longitudinal integral length scale.

The characteristic frequency of the gust wind is computed from the gust duration

$$f = \frac{1}{2 \times 4.1825T} \quad (4)$$

where, f is the characteristic frequency of the gust wind.

With the characteristic frequency, the wind speeds of the longitudinal component along and across the track are

$$w_x = f \cdot \tilde{x} \cdot \cos(\alpha) \cdot \frac{1}{\bar{w}} \quad (5)$$

$$w_y = f \cdot \tilde{x} \cdot \sin(\alpha) \cdot \frac{1}{\bar{w}} \quad (6)$$

where, w_x is the wind speed of the longitudinal component along the track; w_y is the wind speed of the longitudinal component across the track; \tilde{x} is the distance from the position of the peak gust wind speed, and it can be calculated by,

$$\tilde{x} = v|t - t_m|, \quad t \in [t_3, t_4] \quad (7)$$

where, t_m is the time corresponding to the peak gust wind speed.

The gust wind perpendicular to the track is computed by

$$w = \bar{w} + (G - 1)\bar{w}e^{-\sqrt{25w_x^2 + 256w_y^2}} \quad (8)$$

The gust wind speed is to be low-pass filtered through the approach of moving spatial average. The window size is the length of a vehicle, and the spatial step size should be smaller than 0.5 m [EN 14067-6 (2010)].

3 Computational algorithms of aerodynamic loads

Fig. 3 gives the velocity diagram of the vehicle speed v , wind speed w and wind angle α . The wind speed relative to the vehicle is defined as synthetic wind speed u , and the angle between the synthetic wind speed and the track is defined as yaw angle β .

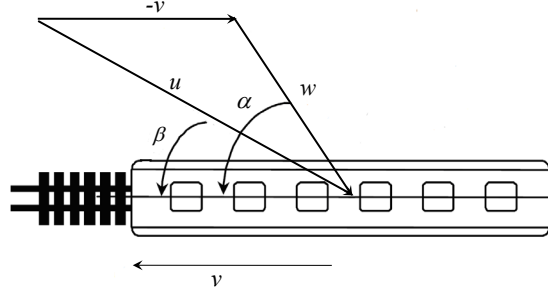


Figure 3: Velocity vectors

The synthetic wind speed and yaw angle are given by

$$u^2(t) = (v(t) + w(t)\cos\alpha)^2 + (w(t)\sin\alpha)^2 \quad (9)$$

$$\beta(t) = \text{atan} \frac{w(t)\sin\alpha}{v + w(t)\cos\alpha} \quad (10)$$

The aerodynamic force and moment can be expressed by the aerodynamic force coefficient and moment coefficient as follows

$$F = \frac{1}{2} \rho A C_F(\beta) u^2 \quad (11)$$

$$M = \frac{1}{2} \rho A h C_M(\beta) u^2 \quad (12)$$

where, F and M are aerodynamic force and moment, respectively; C_F and C_M are force coefficient and moment coefficient, respectively; ρ is air density; A is reference area, $A=10 \text{ m}^2$; h is reference height, $h=3 \text{ m}$.

The aerodynamic force coefficient $C_F(\beta)$ and aerodynamic moment coefficient $C_M(\beta)$ can be determined by the wind tunnel test or computational fluid dynamic method, for a variety of yaw angles. In the present paper, the numerical wind tunnel method is used to obtain the side force coefficient C_{Fs} , lift force coefficient C_{Fl} , rolling moment coefficient C_{Mr} , yaw moment coefficient C_{My} , and pitch moment coefficient C_{Mp} of a high-speed train, see Fig. 4 [Yu, Zhang and Zhang (2012); Yu, Jiang, Zhang et al. (2019)].

For the gust wind model, the gust wind speed is a function of time, thus the synthetic wind speed u and yaw angle β are instantaneous variables. Based on the quasi-steady theory, the fluctuations of aerodynamic loads are consistent with the wind fluctuations [EN 14067-6 (2010); Li, Zhang, Zou et al. (2014); Yu, Jiang, Zhang et al. (2019)]. The aerodynamic force and moment are respectively evaluated by the following equations,

$$F(t) = \frac{1}{2} \rho A C_F(\beta(t)) u^2(t) \quad (13)$$

$$M(t) = \frac{1}{2} \rho A h C_M(\beta(t)) u^2(t) \quad (14)$$

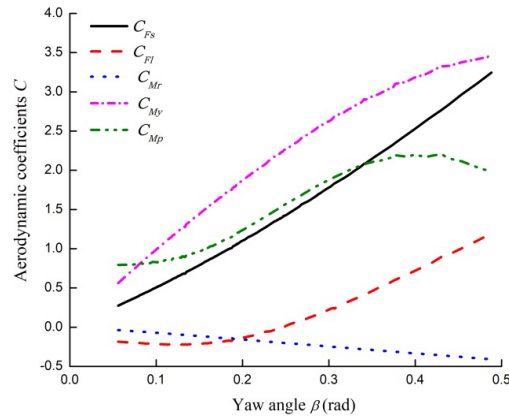


Figure 4: Aerodynamic coefficients

4 Vehicle system dynamic model

The commercial software SIMPACK is used to set up a vehicle system dynamic model, which is shown in Fig. 5. The carbody, bogies, wheelsets, etc., are considered as rigid bodies, and the whole vehicle system dynamic model has 50 degrees of freedoms [Yu, Liu, Liu et al. (2016)]. The bogie and wheelsets are connected by the first suspension system, and the carbody and bogie are connected by the secondary suspension system. The suspension system in the vehicle system dynamic model is constructed with force elements. As to the wheel-rail contact, the worn profile tread and T60 Rail are used. A measured track irregularity of an actual Chinese high-speed railway is used in this study.

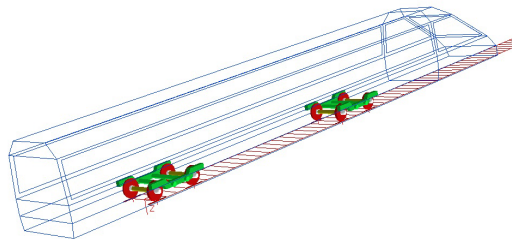


Figure 5: Vehicle dynamic model

The aerodynamic loads, which have been depicted in Section 3, are input into the vehicle dynamic model to conduct dynamic simulation. The operational safety characteristics of a railway vehicle can be evaluated in terms of characteristic wind curves (CWC), which is defined as the critical wind speed causing the vehicle to exceed the limit value of the operational safety index for each train speed. The load reduction factor is widely used by researchers because it is accessible and can be obtained from measured wheel force data [EN 14067-6 (2010); Yu (2014); Yu, Liu, Liu et al. (2016)], which is

$$\Delta P / \bar{P} < 0.8 \quad (15)$$

where ΔP is reduction amount of vertical wheel load, and \bar{P} is average vertical wheel load of the left and right wheel. The load reduction factor shall be 2 Hz low-pass filtered.

5 Numerical computation analysis

In the simulation, the train speed is 200 km/h, 250 km/h, 300 km/h, 350 km/h and 400 km/h, the mean wind speed is 10 m/s, 15 m/s, 20 m/s, 25 m/s and 30 m/s, the wind angle is 30° , 60° , 90° , 120° , and 150° , respectively. A symmetrical gust wind model was established in the present paper, and $t_1=3$ s, $t_2=5$ s, $t_3=10$ s, $t_m=15$ s, $t_4=20$ s, $t_5=25$ s, $t_6=27$ s, $t_7=30$ s.

Fig. 6 shows the gust wind under different wind angles for the mean wind speed of 20 m/s, the y -coordinate is the ratio of the gust wind speed to the mean wind speed, which can reflect the fluctuation of the wind. As shown in Fig. 6, the peak value of the gust wind corresponding to the wind angle of 90° has minimum value. As the wind angle is farther away from 90° , the ratio of the peak wind speed to the mean value becomes larger. In addition, as is shown in Eqs. (8), (9) and (11), the gust wind time histories are the same with respect to the two wind angles of 90° symmetry. What should be noticed is that, the simulated peak value is smaller than the theoretical peak value \hat{w} (the corresponding ratio is 1.6946) as a result of filtering.

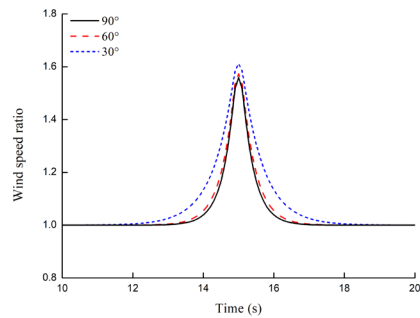


Figure 6: Wind speed ratio under different wind angles

Fig. 7 shows the gust wind under different mean wind speeds for the wind angle of 90° , the y -coordinate is the same as that of Fig. 6. It can be seen from Fig. 7 that, the ratio of the peak wind speed to the mean value becomes larger with the increasing of the mean wind speed.

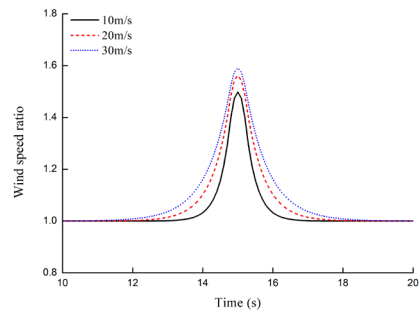


Figure 7: Wind speed ratio under different mean wind speeds

Fig. 8 shows the aerodynamic side force for a variety of wind angles, when the train speed is 300 km/h and the mean wind speed is 20 m/s. The y -coordinate is the ratio of the

side force to the mean value. As shown in Fig. 8, when the wind angle swings to 0° , the ratio of the peak side force to the mean becomes larger. What should be noticed is that, as the mean side forces for each wind angle are different, the side force corresponding to the wind angle of 90° reach the maximum, the descending order of side force for each wind angle is 90° - 60° - 120° - 30° - 150° , as shown in Fig. 9.

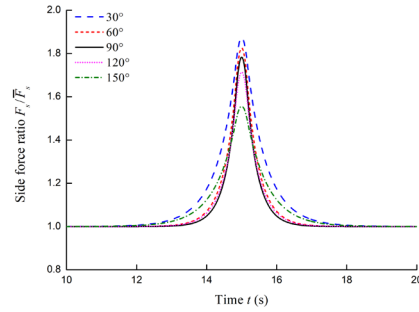


Figure 8: Aerodynamic side force ratio under different wind angles

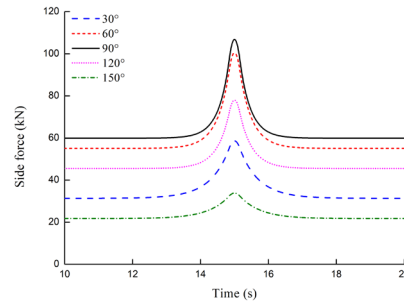


Figure 9: Aerodynamic side force under different wind angles

Fig. 10 shows the aerodynamic side force under different mean wind speeds when the train speed is 300 km/h and the wind angle is 90° , the y -coordinate is the same as that of Fig. 8. As is illustrated in Fig. 10, the ratio of the peak side force to the mean value becomes larger when the mean wind speed increases.

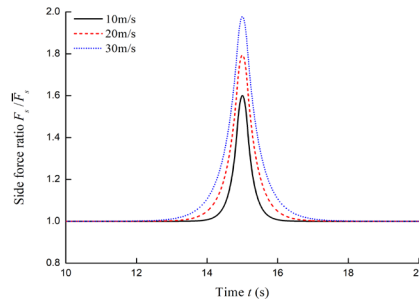


Figure 10: Aerodynamic side force ratio under different mean wind speeds

Fig. 11 shows the load reduction factor under different wind angles when the train speed

is 300 km/h and the mean wind speed is 20 m/s. As shown in Fig. 11, the wind angle has great influence on the load reduction factor, which reaches the maximum when the wind angle is 90°, and the descending order of the load reduction factor for each wind angle is 90°-60°-120°-30°-150°. From Fig. 11, the worst condition occurs when the wind angle reaches somewhere around 90°. Thus, the pure crosswind, i.e., the wind angle of 90° is mainly considered below.

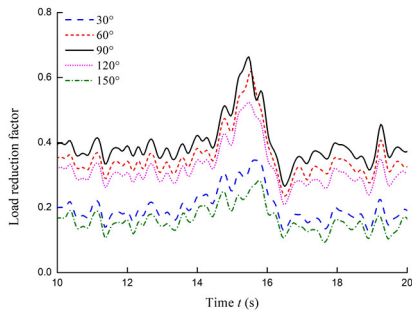


Figure 11: Safety index-wind angle

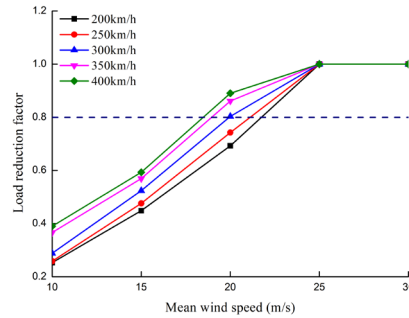


Figure 12: Safety index-mean wind speed

Fig. 12 shows the load reduction factor under different mean wind speeds and train speeds for the wind angle of 90°, the horizontal dash line corresponds to the limit of load reduction factor. As shown in Fig. 12, the load reduction increases with the increasing of the mean wind speed and the train speed. The intersection points of the dash line with each curve can be obtained, which indicates the maximum allowable wind speed that the train can withstand. Therefore, the CWC of the high-speed train exposed to gust wind can be obtained, which is shown in Fig. 13.

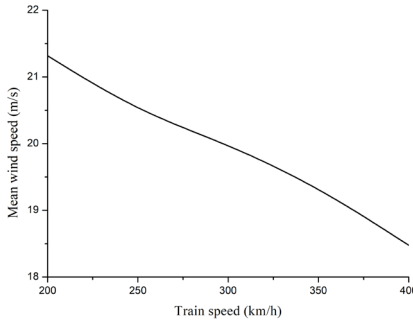


Figure 13: CWC

However, some parameters in the wind-train system are difficult to measure and have a relatively low level of accuracy. Therefore, in this paper, the impact of the gust factor, gust duration, and aerodynamic coefficients on the critical wind speed of the high-speed train exposed to gust wind are examined. Fig. 14 shows the influence of each system parameter on the ratio of the critical wind speed when the train speed is 300 km/h and the wind angle is 90°. The values of each system parameter are changed individually from -10% to 10% (5% intervals), and the critical wind speed ratio on the vertical axis is

defined as the ratio of the critical wind speeds corresponding to uncertain system parameters to the ones corresponding to the original system parameters.

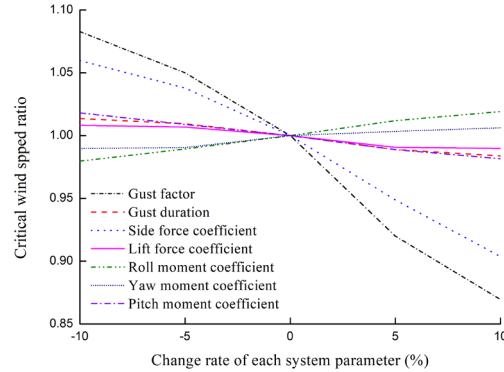


Figure 14: Influence of system parameter on critical wind speed ratio

From Fig. 14, the gust factor has the most significant influence on the critical wind speed ratio, followed by the aerodynamic side force coefficient, while other system parameters have relatively small influence. Within the range of -10% to 10%, the critical wind speed ratio shows certain nonlinear characteristics for the gust factor and side force coefficient, and almost linear relation for the other system parameters studied in this paper. Therefore, due to the relatively low precision for measurement or CFD calculation, the gust factor and aerodynamic side force coefficient require great concern when performing operational safety assessment of railway vehicle subjected to strong gust wind.

6 Conclusions

Crosswind stability of the railway vehicle has caused much concern in recent years. In the present paper, a typical gust wind model for any wind direction is constructed to study the operational safety characteristics of the high-speed train. In addition, the influence of system parameters, such as the gust factor, gust duration and aerodynamic coefficients, on the operational safety of the high-speed train is studied. According to the simulation results, the conclusions are as follows:

- (1) The ratio of peak value to mean value of the wind speed increases when the mean wind speed increases or the wind angle swings far away from 90° .
- (2) The descending order of the operational safety index of the train for various wind angles is 90° - 60° - 120° - 30° - 150° , and the worst condition occurs when the wind angle reaches around 90° .
- (3) The gust factor and aerodynamic side force coefficient have significant impact on critical wind speed, while the gust duration, lift force coefficient and aerodynamic moment coefficient have relatively small impact on critical wind speed. The gust factor and aerodynamic side force coefficient require great attention when performing operational safety assessment of a railway vehicle subjected to strong gust wind.

Acknowledgement: The paper is supported by the National Natural Science Foundation of China (Grant No. 51705267), China Postdoctoral Science Foundation Grant (Grant No. 2018M630750), National Natural Science Foundation of China (Grant No. 51605397), Natural Science Foundation of Shandong Province, China (Grant No. ZR2014EEP002).

Conflicts of Interest: The authors declare that they have no conflicts of interest to report regarding the present study.

References

- Cheli, F.; Ripamonti, F.; Rocchi, G.** (2010): Aerodynamic behaviour investigation of the new EMUV250 train to cross wind. *Journal of Wind Engineering and Industrial Aerodynamics*, vol. 98, pp. 189-201.
- Chen, X. D.; Xu, Y. G.** (2014): Numerical study on the running safety of high-speed train under the cross wind. *Applied Mechanics and Materials*, vol. 694, pp. 109-113.
- Dorigatti, F.; Sterling, M.; Baker, C. J.; Quinn, A. D.** (2015): Crosswind effects on the stability of a model passenger train-A comparison of static and moving experiments. *Journal of Wind Engineering and Industrial Aerodynamics*, vol. 138, pp. 36-51.
- EN 14067-6** (2010): Railway applications-Aerodynamics-Part 6: requirements and test procedures for cross wind assessment. CEN, Brussels.
- Giappino, S.; Rocchi, D.; Schito, P.; Tomasini, G.** (2016): Cross wind and rollover risk on lightweight railway vehicles. *Journal of Wind Engineering and Industrial Aerodynamics*, vol. 153, pp. 106-112.
- Kikuchi, K., Suzuki, M.** (2015): Study of aerodynamic coefficients used to estimate critical wind speed for vehicle overturning. *Journal of Wind Engineering and Industrial Aerodynamics*, vol. 147, pp. 1-17.
- Kozmar, H.; Butler, K.; Kareem, A.** (2012): Transient cross-wind aerodynamic loads on a generic vehicle due to bora gusts. *Journal of Wind Engineering and Industrial Aerodynamics*, vol. 111, pp. 73-84.
- Li, T.; Zhang, J. Y.; Zou, Y. S.; Zhang, W. H.** (2014). Dynamic performances of high-speed train in wind shear, *Frontiers in Aerospace Engineering*, vol. 3, no. 1, pp. 17-22.
- Lv, G. Y.** (2016): Research on high-speed train operation safety in the gust environment. Dalian: Dalian Jiaotong University (In Chinese).
- Mao, J.; Xi, Y. H.; Gao, L.; Yang, G. W.** (2014): Aerodynamic drag of a high-speed train under cross wind conditions. *Journal of Central South University (Science and Technology)*, vol. 45, no. 11, pp. 4059-4067 (In Chinese).
- Munoz-Paniagua, J.; García, J.; Lehueur, B.** (2017): Evaluation of RANS, SAS and IDDES models for the simulation of the flow around a high-speed train subjected to crosswind. *Journal of Wind Engineering & Industrial Aerodynamics*, vol. 171, pp. 50-66.
- Yan, N. J.; Chen, X. Z.; Li, Y. L.** (2018): Assessment of overturning risk of high-speed trains in strong crosswinds using spectral analysis approach. *Journal of Wind Engineering & Industrial Aerodynamics*, vol. 174, pp. 103-118.

Yu, M. G. (2014): Study on the wind-induced safety of the high-speed train based on the reliability. Chengdu: Southwest Jiaotong University (In Chinese).

Yu, M. G.; Jiang, R. C.; Zhang, Q.; Zhang, J. Y. (2019): Crosswind stability evaluation of high-speed train using different wind models. *Chinese Journal of Mechanical Engineering*, vol. 32, no. 40.

Yu, M. G.; Liu, J. L.; Liu, D. W.; Chen, H. M.; Zhang, J. Y. (2016): Investigation of aerodynamic effects on the high-speed train exposed to longitudinal and lateral wind velocities. *Journal of Fluids and Structures*, vol. 61, pp. 347-361.

Yu, M. G.; Zhang, J. Y.; Zhang, W. H. (2012): Unsteady aerodynamic loads of high-speed trains under stochastic winds. *Journal of Mechanical Engineering*, vol. 48, no. 20, pp. 113-120 (In Chinese).